Supporting Information for

Spin Coherence and Magnetization Dynamics of $TMA_2[KCo_{1-x}Fe_x(CN)_6]$ toward Coordination-Framework Spin Qubits

Shraddha Gupta,[a,b]* Masanori Wakizaka,[c]* Takeshi Yamane,[d] Kazunobu Sato,[d*] Ryuta Ishikawa,[e] Nobuto Funakoshi,[b] and Masahiro Yamashita[a,b]*

[a] School of Chemical Science and Engineering, Tongji University, Siping Road 1239, Shanghai 200092, P, R, China

[b] Department of Chemistry, Graduate School of Science, Tohoku University, 6-3 Aramaki-Aza-Aoba, Aoba-Ku, Sendai 980-8578, Japan.

[c] Department of Applied Chemistry and Bioscience, Faculty of Science and Technology, Chitose Institute of Science and Technology, 758-65 Bibi, Chitose 066-8655, Japan.

[d] Department of Chemistry, Graduate School of Science, Osaka Metropolitan University, 3-3-138 Sugimoto, Sumiyoshi-Ku, Osaka 558-8585, Japan.

[e] Department of Chemistry, Faculty of Science, Fukuoka University, Nanakuma 8-19-1, Fukuoka 814-0180, Japan.

E-mail: shraddha.gupta.q7@alumni.tohoku.ac.jp, ma-wakiz@photon.chitose.ac.jp,

sato@omu.ac.jp, masahiro.yamashita.c5@tohoku.ac.jp

Contents

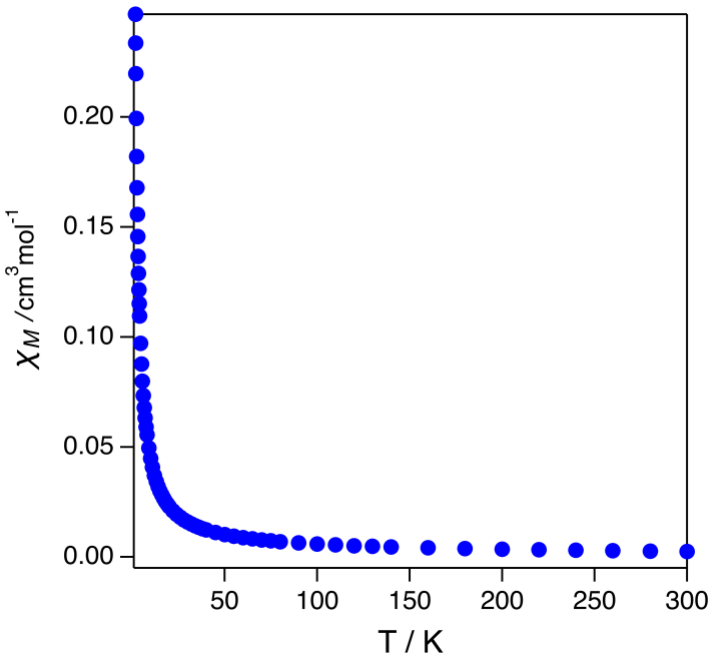

Figure S1: χ_m–*T* plot of $(TMA)_2[KFe(CN)_6]$.

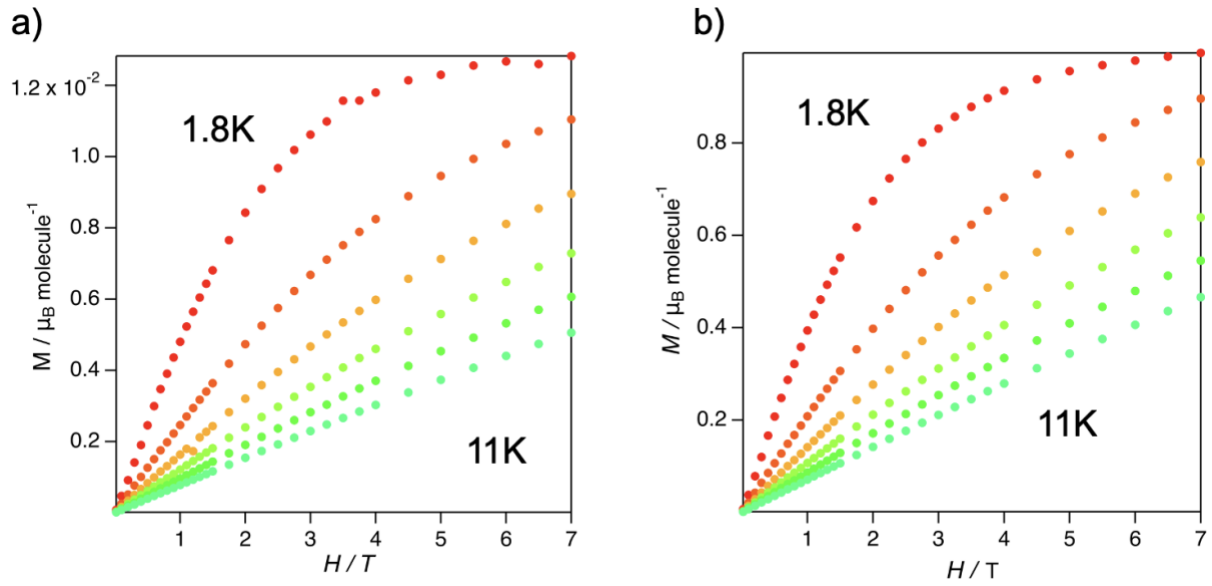

Figure S2 : Temperature dependence of *M*–*H* curves, a) Fe (2%) / Co coordination-framework, b) Fe (100%) coordination-framework.

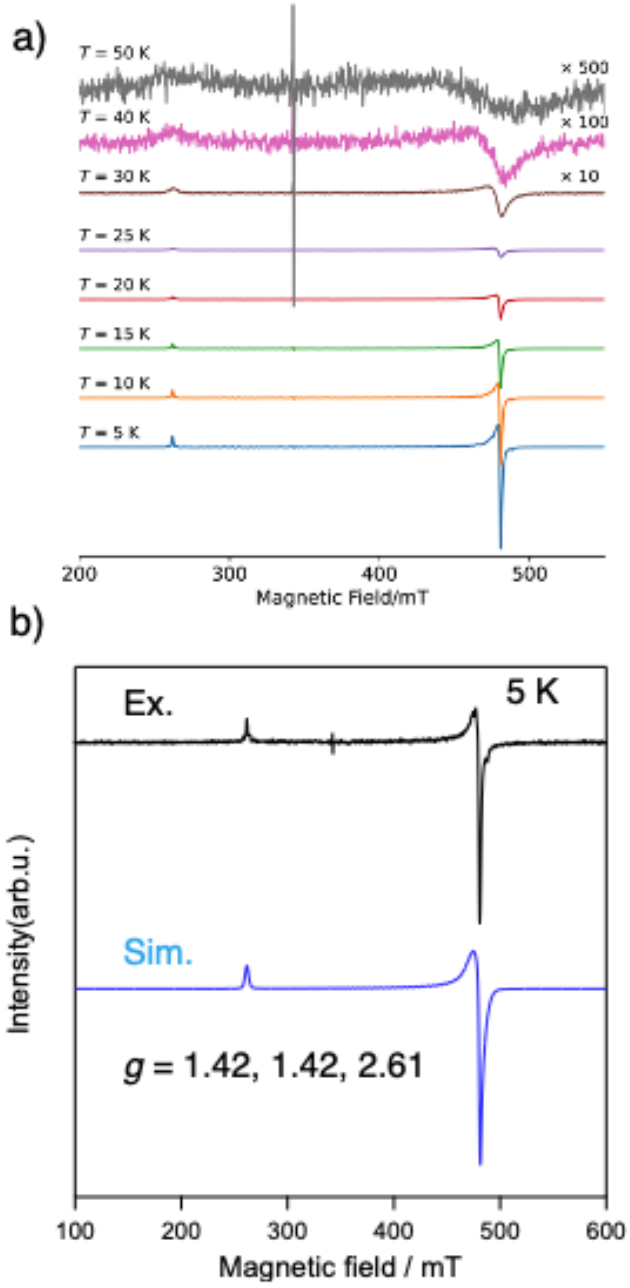

Figure S3: a) Temperature dependence of powder-pattern EPR spectra of $TMA_2[KCo_{0.98}Fe_{0.02}(CN)_6]$ [MW freq.: 9.54634 GHz, MW power: 0.02 mW]. b) Comparison with the simulated one using EasySpin: g = 1.418, 1.419, and 2.606; g_{Strain} = 0, 0.04, and 0.03; lwpp = 0.8 (Gaussian) and 0.8 (Lorentzian).

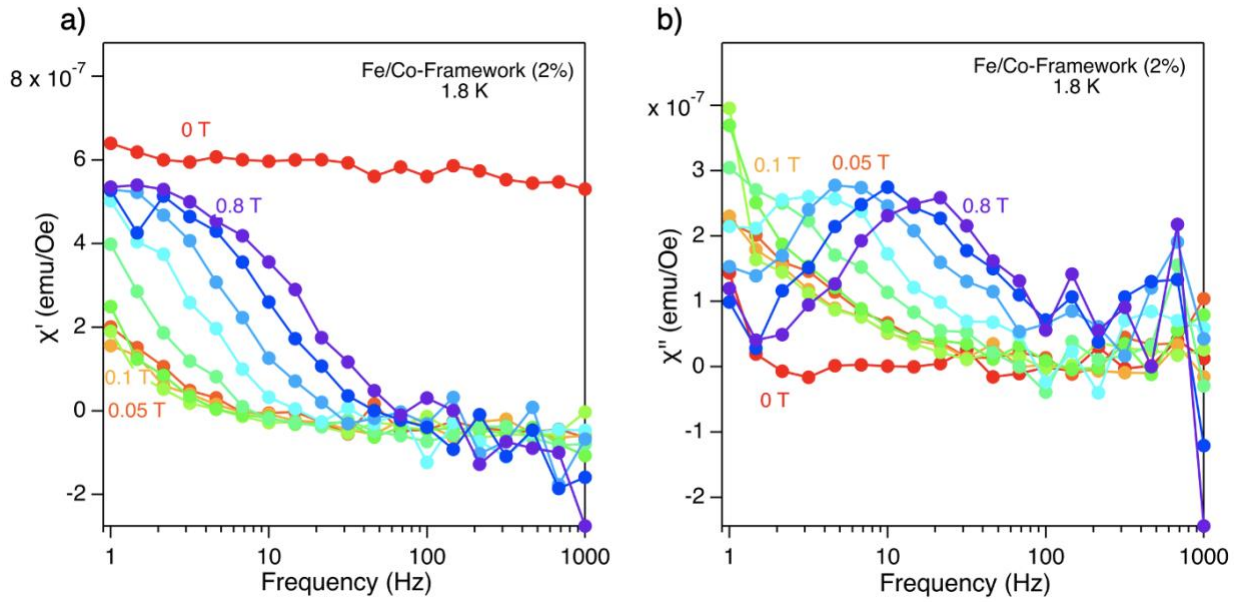

Figure S4. (a) The real part (χ') and (b) the imaginary part (χ'') of AC susceptibility of $TMA_2[KCo_{0.98}Fe_{0.02}(CN)_6]$, measured at 1.8 K under magnetic field of 0, 0.05, 0.1, 0.2, 0.3, 0.4, 0.5, 0.6, 0.7, 0.8 T. AC drive is 2.5 Oe.

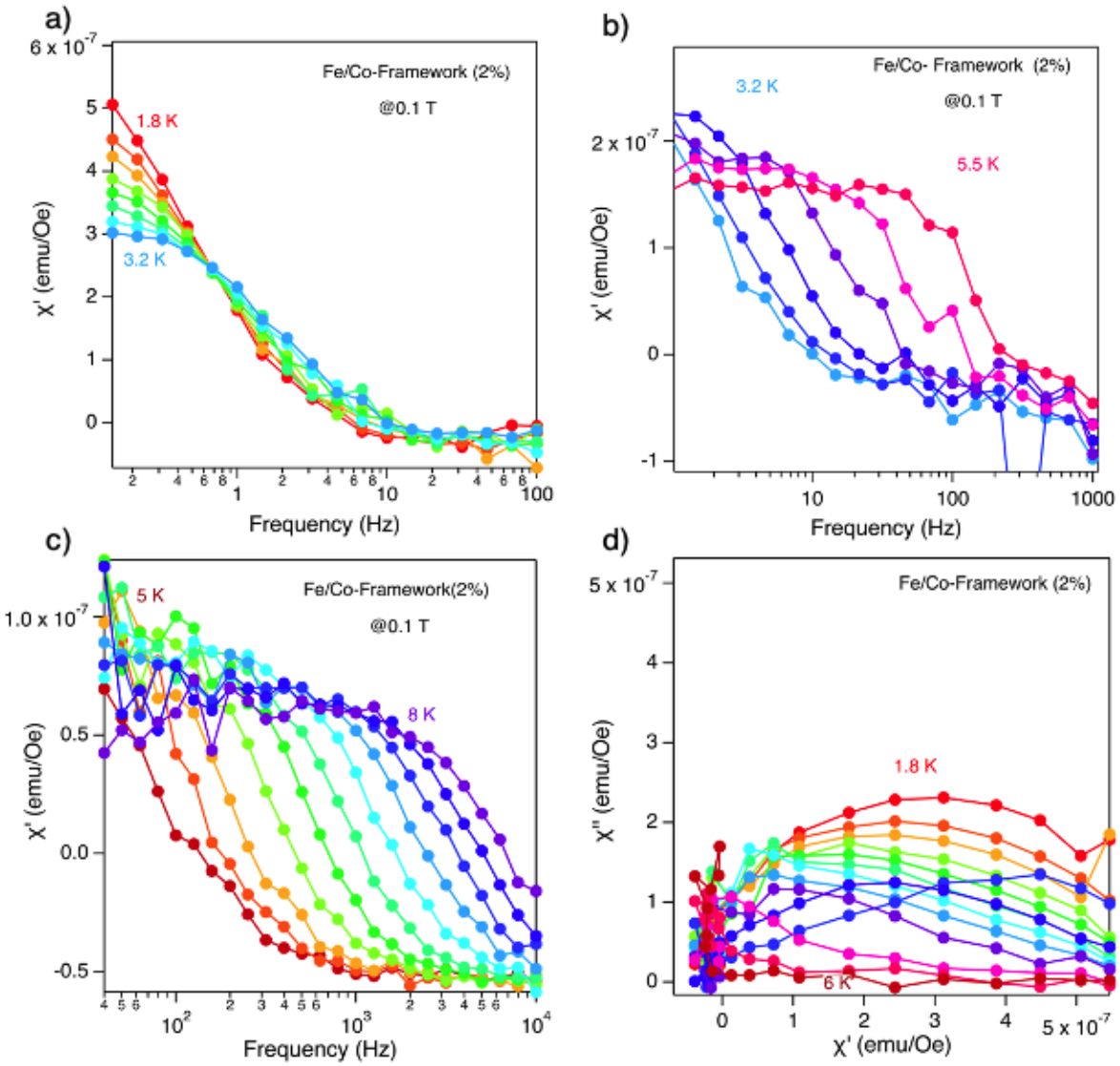

Figure S5. a-c) The real part of the AC susceptibility (χ') of $TMA_2[KCo_{0.98}Fe_{0.02}(CN)_6]$, measured at 1.8, 2, 2.2, 2.4, 2.6, 2.8, 3, 3.2, 3.5, 4, 4.5, 5, 5.3, 5.6, 5.9, 6.2, 6.5, 6.8, 7.1, 7.4, 7.7, 8K over a range of 0.1–1000 Hz under a static magnetic field of 0.1 T. d) the Cole-Cole plot.

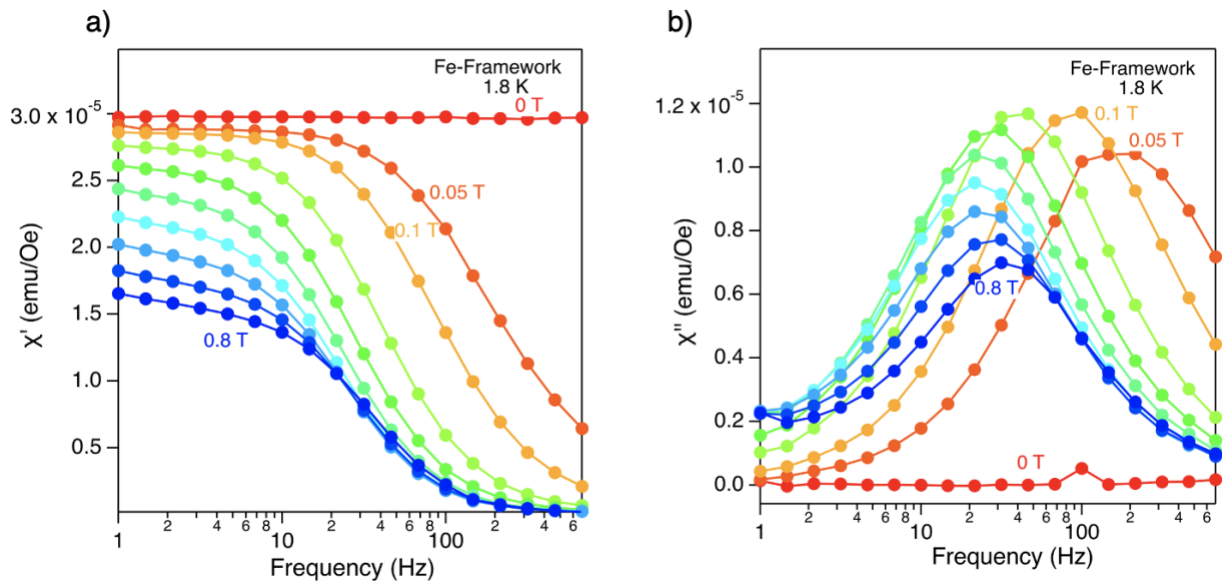

Figure S6. (a) The real part (χ') and (b) the imaginary part (χ'') of AC susceptibility of $TMA_2[KFe(CN)_6]$, measured at 1.8 K under magnetic field of 0, 0.05, 0.1, 0.2, 0.3, 0.4, 0.5, 0.6, 0.7, 0.8 T. AC drive is 2.5 Oe.

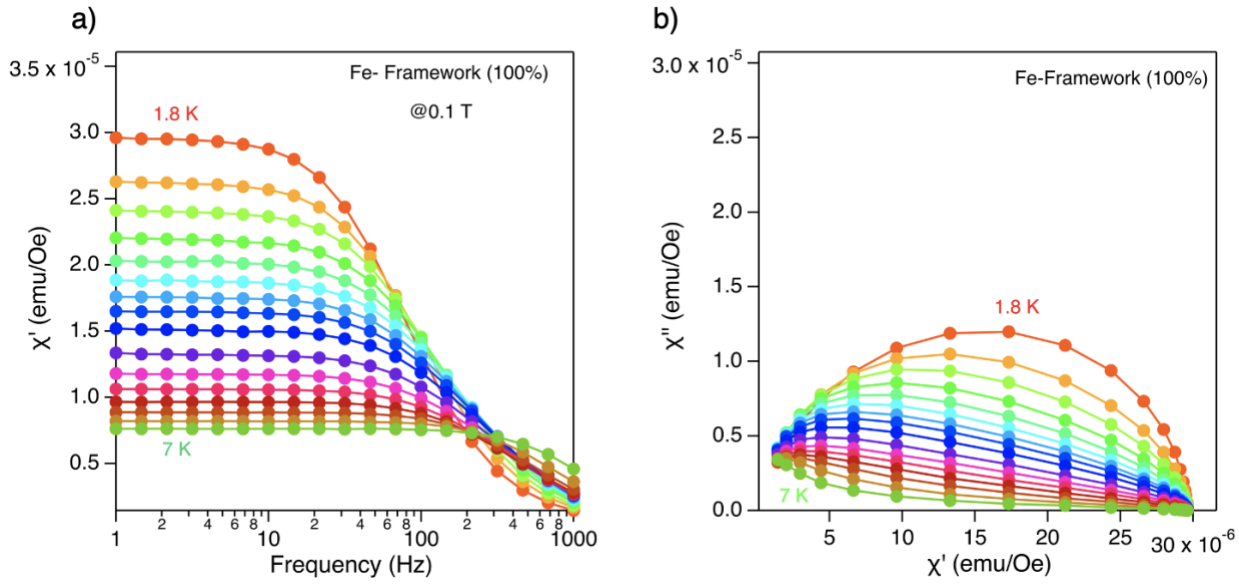

Figure S7. a) The real part of the AC susceptibility (χ') of $TMA_2[KFe(CN)_6]$, measured at 1.8, 2, 2.2, 2.4, 2.6, 2.8, 3, 3.2, 3.5, 4, 4.5, 5, 5.3, 5.6, 5.9, 6.2, 6.5, 6.8, 7.1, 7.4, 7.7, 8K over a range of 0.1–1000 Hz under a static magnetic field of 0.1 T.) the Cole-Cole plot.

Table S1. Summary of AC susceptibility fitting parameters of Fe-Framework (100 %) under 0.1 T

T [K]	$\chi_T - \chi_S$ [emu Oe^{-1}]	τ [s]	α	$\sigma\,\chi_T - \chi_S$ [emu Oe^{-1}]	$\sigma\,\tau$ [s]	$\sigma\,\alpha$
1.8	2.93E-05	0.0018854	0.11625	2.25E-07	2.29E-05	6.39E-03
2	2.61E-05	0.001435	0.12964	1.86E-07	1.64E-05	5.96E-03
2.2	2.40E-05	0.0011965	0.14046	1.91E-07	1.53E-05	6.61E-03
2.4	2.20E-05	0.0010064	0.14908	2.10E-07	1.55E-05	7.90E-03
2.6	2.02E-05	0.00087961	0.15348	2.11E-07	1.48E-05	8.57E-03
2.8	1.89E-05	0.00078162	0.16425	2.00E-07	1.35E-05	8.60E-03
3	1.76E-05	0.00071368	0.16565	2.01E-07	1.33E-05	9.25E-03
3.2	1.66E-05	0.00065291	0.17182	2.04E-07	1.32E-05	9.81E-03
3.5	1.51E-05	0.00059007	0.17421	2.00E-07	1.29E-05	1.05E-02
4	1.32E-05	0.00051278	0.17273	1.96E-07	1.26E-05	1.15E-02
4.5	1.16E-05	0.00046259	0.16394	1.86E-07	1.21E-05	1.23E-02
5	5.62E-06	0.00032	0.21958	5.08E-08	5.07E-06	0.00738
5.3	5.288E-06	0.00030042	0.20734	4.84E-08	0.00000469	0.00751
5.6	4.985E-06	0.00027358	0.19208	4.54E-08	0.00000419	0.00753
5.9	4.686E-06	0.00024102	0.17074	3.9E-08	0.0000033	0.00693
6.2	4.412E-06	0.00020615	0.14546	3.72E-08	0.00000278	0.00707
6.5	4.161E-06	0.00016986	0.11755	3.38E-08	0.00000213	0.00687
6.8	3.954E-06	0.000136	0.094842	2.58E-08	0.00000132	0.00556
7.1	3.757E-06	0.00010554	0.072787	2.1E-08	8.43E-07	0.00477
7.4	3.581E-06	8.0266E-05	0.055601	1.86E-08	5.75E-07	0.00445
7.7	3.425E-06	6.0166E-05	0.043698	1.54E-08	3.62E-07	0.00381
8	3.279E-06	4.4964E-05	0.034916	1.15E-08	2.07E-07	0.00289

Table S2. Summary of AC susceptibility fitting parameters of Fe/Co-Framework (2 %) under 0.1 T

T [K]	$\chi_T - \chi_S$ [emu Oe^{-1}]	τ [s]	α	$\sigma\,\chi_T - \chi_S$ [emu Oe^{-1}]	$\sigma\,\tau$ [s]	$\sigma\,\alpha$
1.8	6.89E-07	0.29854	0.24901	1.73E-08	0.0141	0.0184
2	6.01E-07	0.23492	0.2455	1.17E-08	0.0085	0.0148
2.2	5.81E-07	0.20561	0.29527	2.03E-08	0.0144	0.0256
2.4	5.29E-07	0.155572	0.27455	3.53E-08	0.02	0.051
2.6	4.33E-07	0.1624	0.20491	2.61E-08	1.71E-02	0.0485
2.8	4.63E-07	0.09802	0.23083	2.25E-08	8.78E-03	0.0388
3	4.17E-07	0.085603	0.19209	1.60E-08	5.78E-03	0.0313
3.2	3.78E-07	0.075378	0.24267	1.56E-08	5.84E-03	0.0327
3.5	3.6697	0.063351	0.23	2.51E-08	0.0126	0
4	3.21E-07	0.022425	0.23	1.89E-08	0.00353	0
4.5	3.06E-07	0.0069103	0.23	2.10E-08	0.00122	0
5	2.23E-07	0.00265	0.13818	1.74E-08	0.00035	0.0468
5.3	1.87E-07	0.00134	0.0438	8.64E-09	8.26E-05	0.0383
5.6	1.7689E-07	0.00087251	0.065279	6.31E-09	0.0000432	0.0303
5.9	1.6457E-07	0.00047884	0.057434	1.04E-08	0.0000429	0.0541
6.2	1.6953E-07	0.00032861	0.096089	4.58E-09	0.0000133	0.0229
6.5	1.4908E-07	0.00018443	0.034432	5.38E-09	0.00000924	0.0309
6.8	1.7075E-07	0.00011484	0.19193	1.17E-08	0.0000132	0.0564
7.1	1.3542E-07	7.1725E-05	0	5.82E-09	0.00000554	0
7.4	1.2885E-07	5.0881E-05	0.01	5.25E-09	0.00000391	0
7.7	1.4188E-07	3.0755E-05	0.099802	1.26E-08	0.00000417	0.0629
8	1.2067E-07	0.00002562	0	5.94E-09	0.00000253	0

Table S3. Summary of magnetic relaxation fitting parameters under 0.1 T

Sample	B [K s^{-1}]	C [K^m s^{-1}]	m	σB [K s^{-1}]	σC [K^m s^{-1}]	σm
$TMA_2[KCo_{0.98}Fe_{0.02}(CN)_6]$	1.1698	3769.9	8.94	0.16	2.33e+3	0.34

Sample	A [K s^{-1}]	C [K^m s^{-1}]	m	σA [K s^{-1}]	σC [K^m s^{-1}]	σm
$TMA_2[KFe(CN)_6]$	0.0020	4397.3	8.74	4.92e-05	2.94e+03	0.33

Standard deviation (σ)

Table S4. MBS parameter

Fe (%)	d (mm/s)	ΔE_Q (mm/s)	FWHM (mm/s)
100	–0.115(36)	1.193(45)	1.730(69)
2	0.046	0.076	0.265

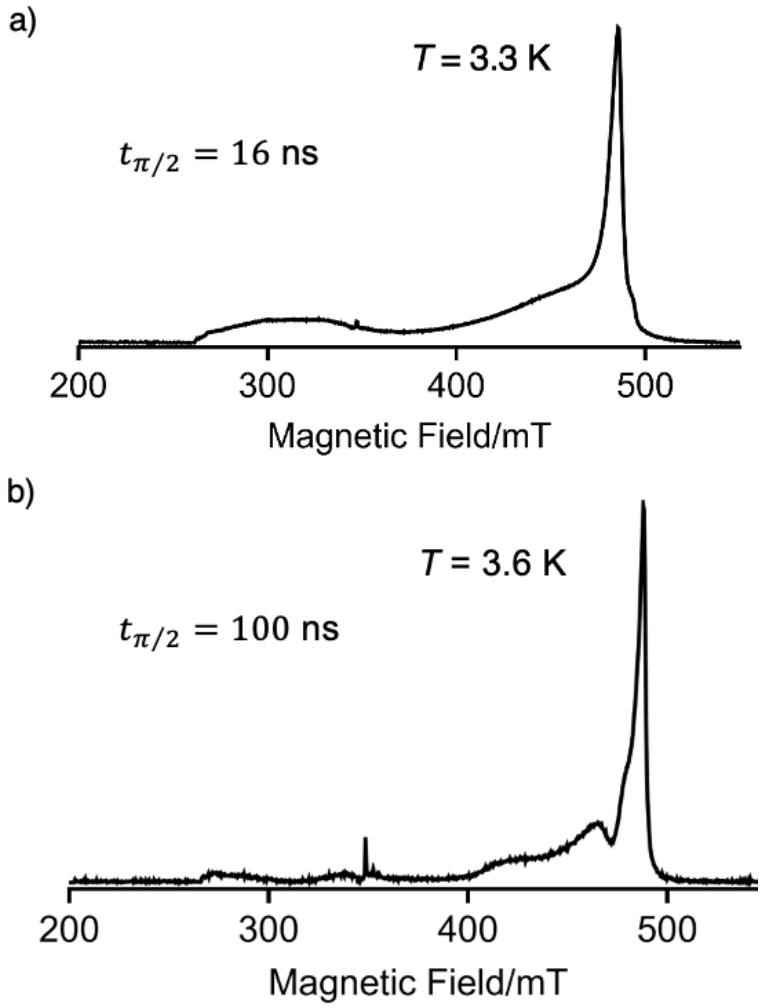

Figure S8: Echo-detected field-swept ESR of a) $TMA_2[KCo_{0.98}Fe_{0.02}(CN)_6]$ and b) $TMA_2[KCo_{0.999}Fe_{0.001}(CN)_6]$ as a function of magnetic field using the MW freq. of 9.68379 GHz for (a) and 9.72389 GHz for (b).

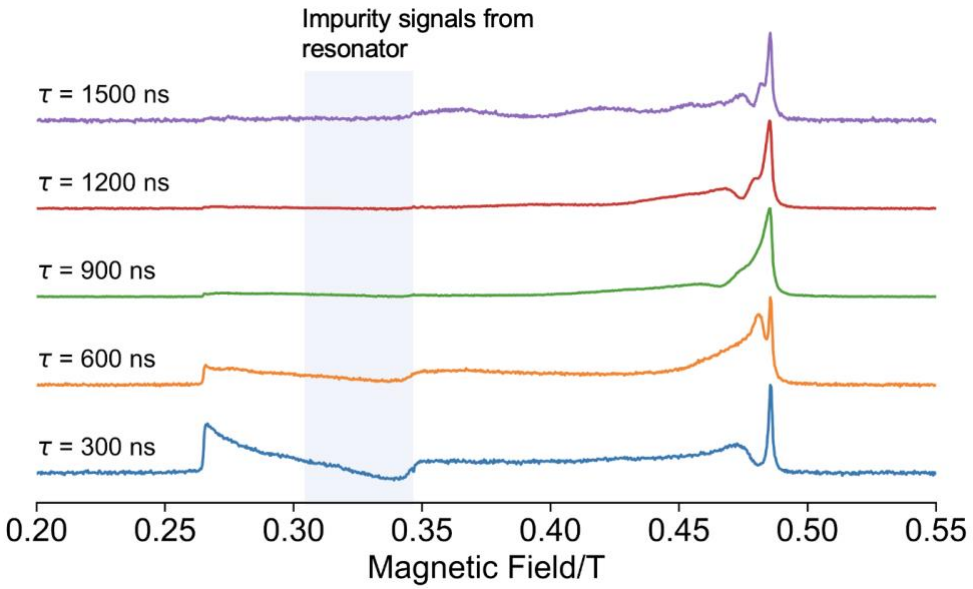

Figure S9: τ dependent ESR spectra of $TMA_2[KCo_{0.999}Fe_{0.001}(CN)_6]$ observed by Hahn-echo detection as a function of magnetic field using the MW freq. of 9.669286 at T = 3.5 K.

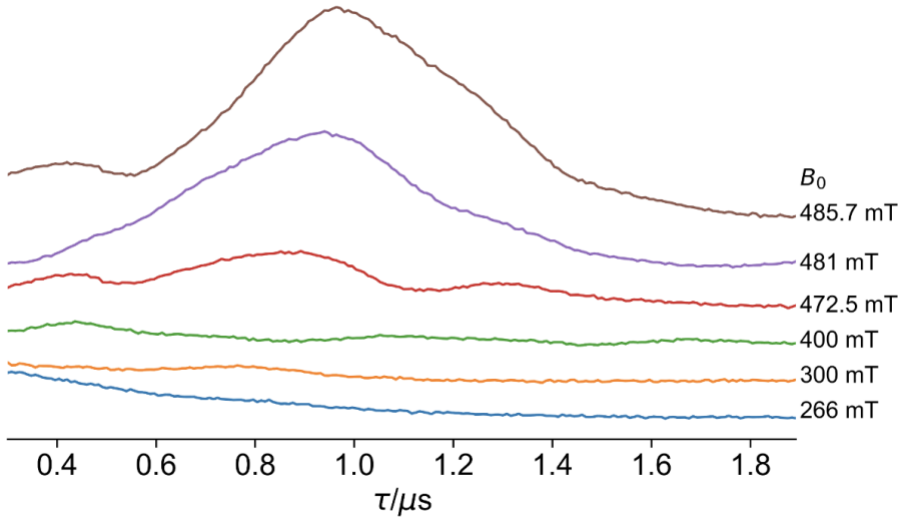

Figure S10: Field dependent two-pulse ESEEM of $TMA_2[KCo_{0.999}Fe_{0.001}(CN)_6]$ observed at 3.5 K.

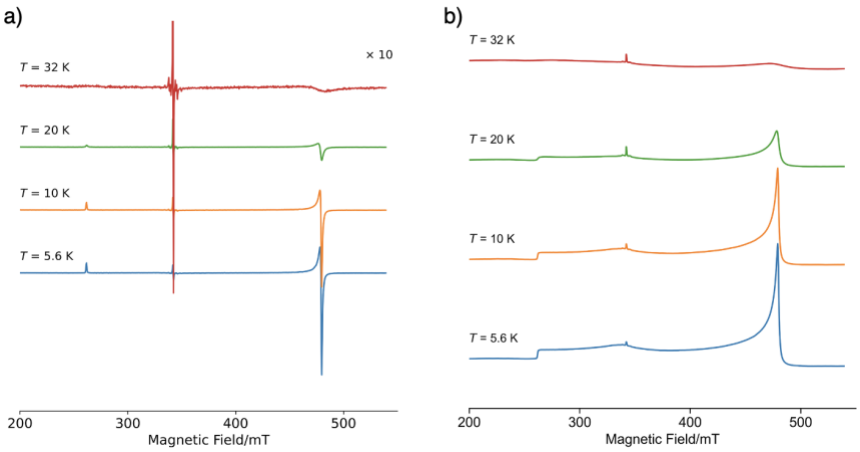

Figure S11: a) Temperature dependence of powder-pattern EPR spectra of $TMA_2[KCo_{0.999}Fe_{0.001}(CN)_6]$ [MW freq.: 9.669286 GHz]. b) Absorption forms of cw-ESR spectra.

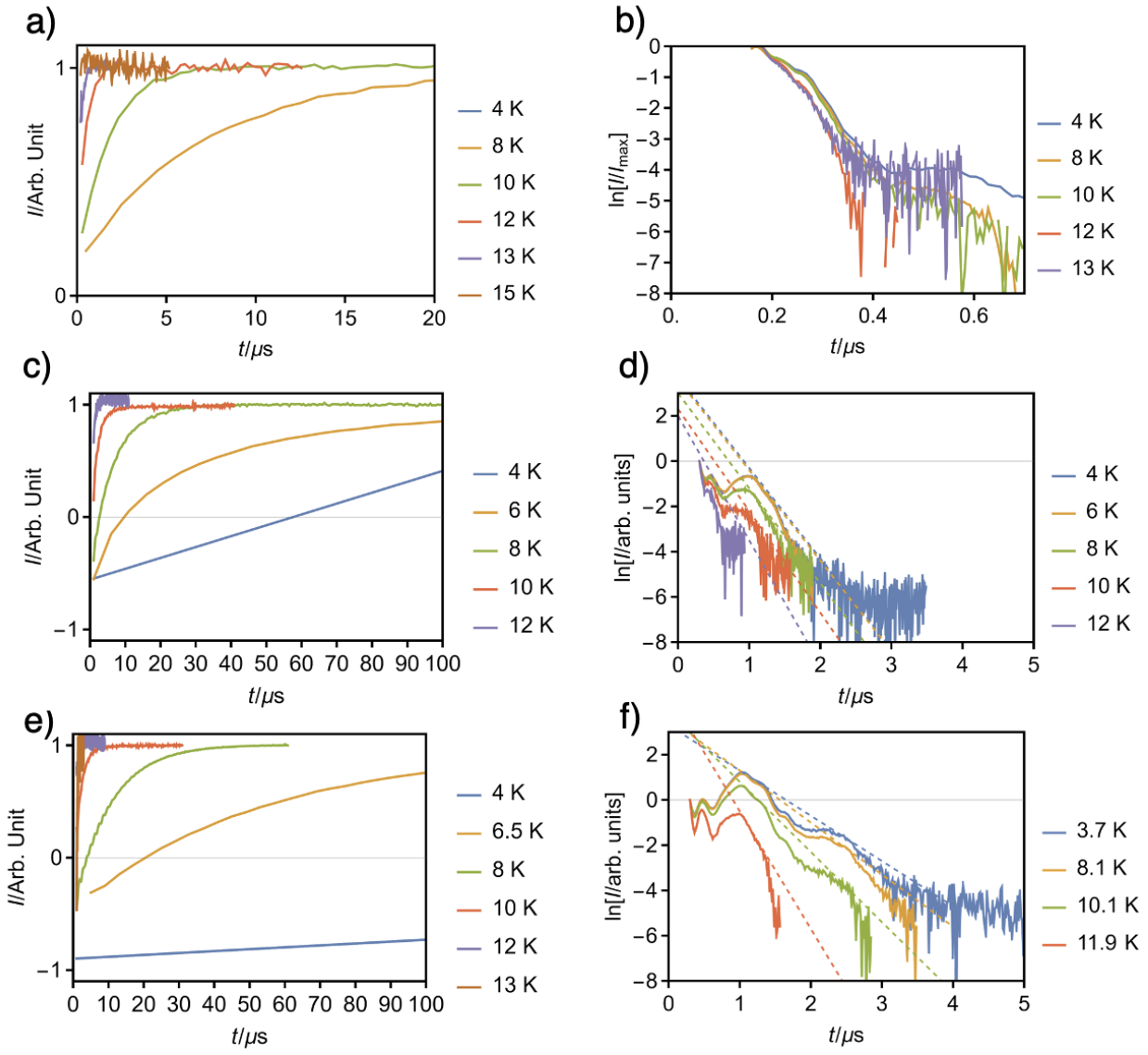

Figure S12: a,c,e) Inversion recovery time (T_1) of $TMA_2[KCo_{0.98}Fe_{0.02}(CN)_6]$ and $TMA_2[KCo_{0.995}Fe_{0.005}(CN)_6]$ and $TMA_2[KCo_{0.999}Fe_{0.001}(CN)_6]$ under a magnetic field of 458.5 mT, 488.25 mT and 488.25 mT respectively. b,d,f) Hahn-echo decay time (T_2) of $TMA_2[KCo_{0.98}Fe_{0.02}(CN)_6]$, $TMA_2[KCo_{0.995}Fe_{0.005}(CN)_6]$ and $TMA_2[KCo_{0.999}Fe_{0.001}(CN)_6]$.

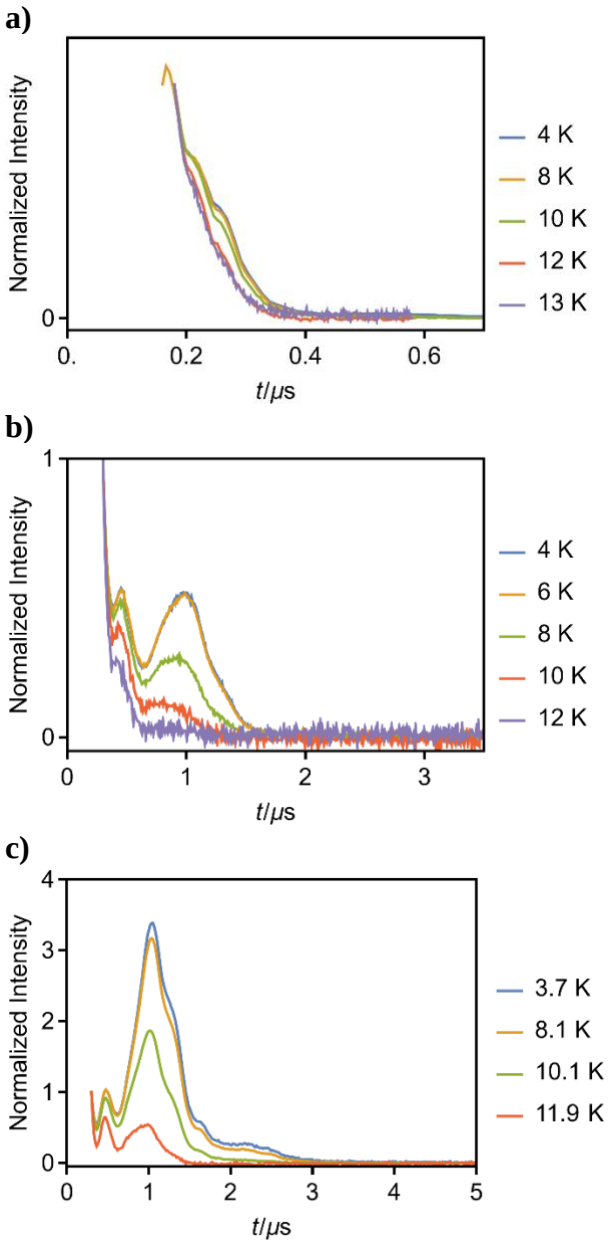

Figure S13: Hahn-echo decay plots of $TMA_2[KCo_{0.98}\ Fe_{0.02}(CN)_6]$ (a), $TMA_2[KCo_{0.995}\ Fe_{0.005}(CN)_6]$ (b) and $TMA_2[KCo_{0.999}\ Fe_{0.001}(CN)_6]$ (c). All the echo decays show drastic initial decays which are due to dephasing in the presence of cross-suppression effects. In (a), the cross-suppression effects dominate to the echo decay.

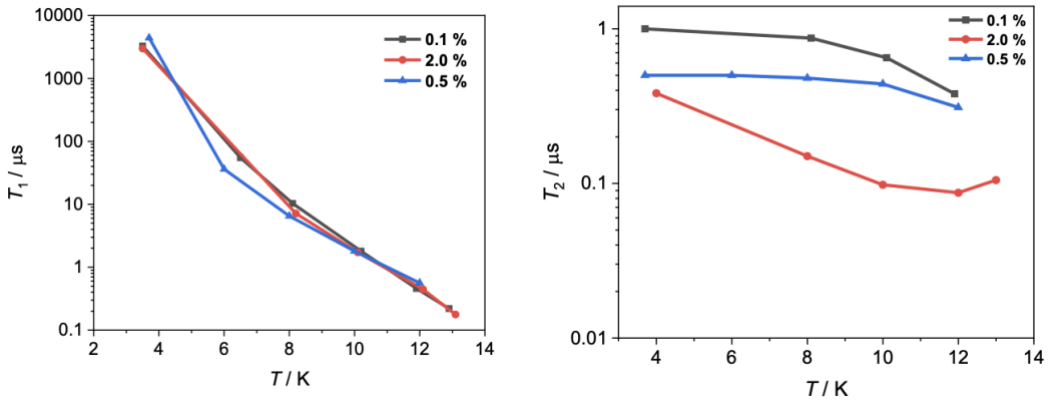

Figure S14. Temperature dependence of (a) the T_1 and (b) T_2 relaxation times of the Fe (0.1, 0.5 and 2 %)/Co coordination-framework.

Table S5. Summary of fitting parameters of $TMA_2[KCo_{0.98}Fe_{0.02}(CN)_6]$ for inversion recovery

T / K	T_1 / µs
3.4	2990
8.2	7.125
10.1	1.721
12.1	0.444
13.1	0.1777

Table S6. Summary of fitting parameters of $TMA_2[KCo_{0.98}Fe_{0.02}(CN)_6]$ for Hahn echo-decay

T / K	T_2 / µs
4	>0.383
8	>0.150
10	>0.098
12	>0.087
13	>0.105

Table S7. Summary of fitting parameters of $TMA_2[KCo_{0.995}Fe_{0.005}(CN)_6]$ for inversion recovery

T / K	T_1 / μs
3.7	4393.7
6	36.1
8	6.5
10	1.8
12	0.56

Table S8. Summary of fitting parameters of $TMA_2[KCo_{0.995}Fe_{0.005}(CN)_6]$ for Hahn echo-decay

T / K	T_2 / μs	**Slope/ μs^{-1}**
3.7	0.5	-4.0
6	0.5	-4.0
8	0.48	-4.2
10	0.44	-4.5
12	0.31	-6.5

Table S9. Summary of fitting parameters of $TMA_2[KCo_{0.999}Fe_{0.001}(CN)_6]$ for inversion recovery

T / K	T_1 / μs
3.5	3268
6.5	54.9
8.1	10.3
10.2	1.8
11.9	0.46
12.9	0.22

Table S10. Summary of fitting parameters of $TMA_2[KCo_{0.999}Fe_{0.001}(CN)_6]$ for Hahn echo-decay

T / K	T_2 / µs	Slope/ μs^{-1}
3.7	1.0	-2.0
8.1	0.87	-2.3
10.1	0.65	-3.1
11.9	0.38	-5.2

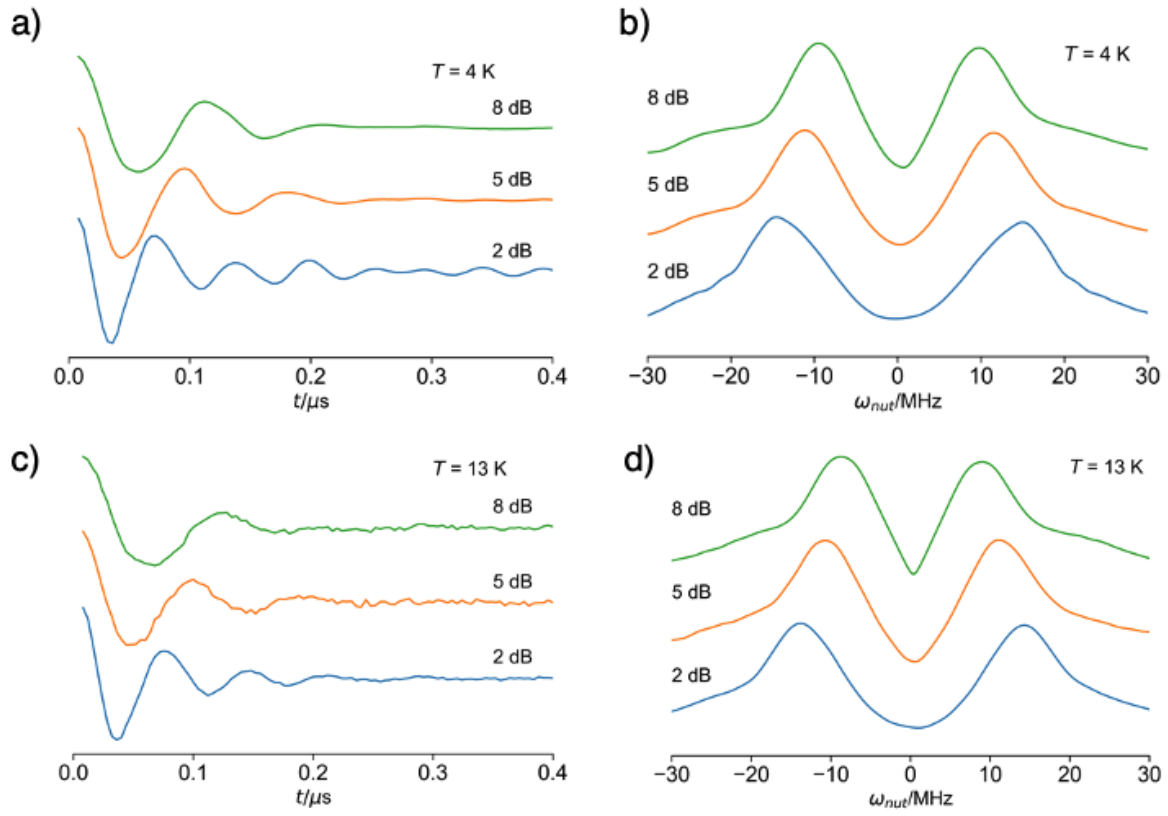

Figure S15: Transient Electron Spin Nutation of $TMA_2[KCo_{0.98}\ Fe_{0.02}(CN)_6]$ at 4 and 13 K.